THE JOURNAL OF BIOLOGICAL CHEMISTRY VOL. 284, NO. 42, pp. 28874–28884, October 16, 2009

A Quantification of Pathway Components Supports a Novel Model of Hedgehog Signal Transduction*[S]

Received for publication, July 22, 2009, and in revised form, August 25, 2009 Published, JBC Papers in Press, August 28, 2009, DOI 10.1074/jbc.M109.041608

Shohreh F. Farzan[‡], Melanie A. Stegman[‡1], Stacey K. Ogden[‡2], Manuel Ascano, Jr.[‡3], Kendall E. Black[‡], Ofelia Tacchelly[‡], and David J. Robbins[‡§4]

From the [‡]Department of Pharmacology and Toxicology, Dartmouth Medical School, Hanover, New Hampshire 03755 and the [§]Norris Cotton Cancer Center, Dartmouth-Hitchcock Medical Center, Lebanon, New Hampshire 03756

The secreted protein Hedgehog (Hh) plays a critical instructional role during metazoan development. In *Drosophila*, Hh signaling is interpreted by a set of conserved, downstream effectors that differentially localize and interact to regulate the stability and activity of the transcription factor Cubitus interruptus. Two essential models that integrate genetic, cell biological, and biochemical information have been proposed to explain how these signaling components relate to one another within the cellular context. As the molar ratios of the signaling effectors required in each of these models are quite different, quantitating the cellular ratio of pathway components could distinguish these two models. Here, we address this important question using a set of purified protein standards to perform a quantitative analysis of *Drosophila* cell lysates for each downstream pathway component. We determine each component's steady-state concentration within a given cell, demonstrate the molar ratio of Hh signaling effectors differs more than two orders of magnitude and that this ratio is conserved *in vivo*. We find that the G-protein-coupled transmembrane protein Smoothened, an activating component, is present in limiting amounts, while a negative pathway regulator, Suppressor of Fused, is present in vast molar excess. Interestingly, despite large differences in the steady-state ratio, all downstream signaling components exist in an equimolar membrane-associated complex. We use these quantitative results to re-evaluate the current models of Hh signaling and now propose a novel model of signaling that accounts for the stoichiometric differences observed between various Hh pathway components.

Hedgehog (Hh)[5] is a developmentally regulated ligand that plays a critical instructional role during embryogenesis (1). The secreted Hh protein signals to neighboring cells, where it specifies cell fate in a concentration-dependent manner by initiating a conserved signaling pathway (1, 2). In addition to its fundamental role in the patterning fields of cells during both vertebrate and invertebrate development, deregulation of the Hh-signaling pathway has also been implicated in a range of human developmental defects and in the promotion of oncogenesis (1, 3–5). Thus, elucidation of the basic mechanisms of Hh signal transduction is essential for the discovery of novel therapeutic targets, which could in turn be modulated to prevent or treat these various human disorders.

In general, Hh is thought to bind to its receptor Patched, a twelve-pass transmembrane protein, relieving its inhibition of Smoothened (Smo) (6–12). Smo is a G-protein-coupled transmembrane protein that is absolutely required for Hh signaling (9, 10, 13). In the absence of Hh, Smo is either inactivated by lysosomal degradation or is found in an intermediate state, where it is actively repressed by Patched (14–16). This repression occurs via an unknown mechanism but results in Smo being transported away from the cell surface and into endosomes (16–18). Upon Hh stimulation, inhibition of Smo is relieved, allowing it to relocalize to the plasma membrane and undergo a conformational change to promote high level signaling (15, 16, 19, 20). Smo signals to a large downstream complex of proteins (HSC), which contains Costal-2 (Cos2), a kinesin-like protein, Fused (Fu), a serine/threonine kinase, and Cubitus interruptus (Ci), a zinc finger transcription factor (21–27). In the absence of Hh, Ci is proteolytically processed to a 75-kDa form, Ci_{75}, which acts as a transcriptional repressor (28). This processing is inhibited in the presence of Hh, resulting in the subsequent accumulation of full-length Ci and, depending upon the strength of the Hh signal, Ci is stabilized, activated, or highly activated, to differentially affect the transcription of a set of target genes (28–31). The additional downstream component Suppressor of Fused (Sufu) is thought to bind to other signaling effectors in a manner that may serve to sequester Ci away from the nucleus (32–35). Other components involved in aspects of Hh signaling are thought to be scaffolded by Cos2, such as protein kinase A, Sgg/GSK3, and CK1, but these accessory proteins are also involved in a variety of other signaling pathways (36–41). A number of models have been proposed for how these various signaling components localize and interact to transduce the Hh signal (42–47). These various models can be simplified into two distinct signaling strategies (see Fig. 1), one in which all of the signaling components are bound directly to Smo in a membrane-associated complex that regu-

* This work was supported, in whole or in part, by National Institutes of Health Grant CA8628 (to D. J. R.). This work was also supported by a Ryan Fellowship (to S. F. F.) and a Rosaline Borison Predoctoral Fellowship (to S. F. F.).

[S] The on-line version of this article (available at http://www.jbc.org) contains supplemental Figs. S1–S6.

[1] Present address: Learning Technology Program, Federation of American Scientists, Washington, D. C. 20036.

[2] Present address: Dept. of Molecular Pharmacology, St. Jude Children's Research Hospital, Memphis, TN 38105.

[3] Present address: Rockefeller University, New York, NY 10065.

[4] To whom correspondence should be addressed: HB 7650, Dartmouth Medical School, Hanover, NH 03755. Tel.: 603-650-1716; Fax: 603-650-1129; E-mail: David.J.Robbins@Dartmouth.edu.

[5] The abbreviations used are: Hh, Hedgehog; Ci, cubitus interruptus; Cos2, Costal-2; Fu, Fused; Sufu, Suppressor of fused; Smo, Smoothened; HSC, Hedgehog signaling complex; HSC-A, HSC-activator complex; HSC-R, HSC-repressor complex; BSA, bovine serum albumin; CI8, Clone-8; HSS, high speed supernatant; HSP, high speed pellet.

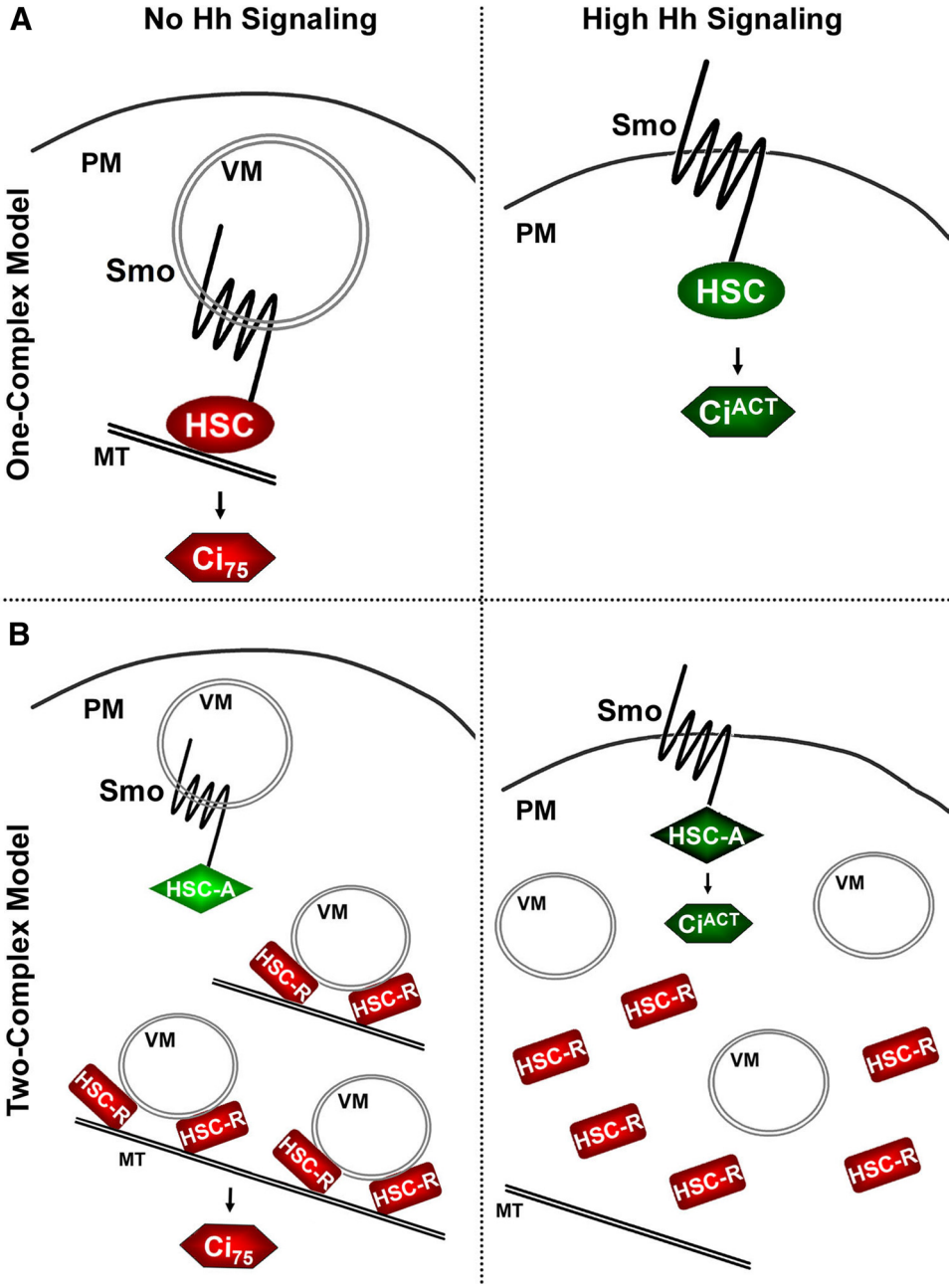

FIGURE 1. **Two current models of Hh signaling.** *A*, one-complex model. *B*, two-complex model. See text for details. *PM*, plasma membrane; *VM*, vesicular membranes; *MT*, microtubules; and *HSC*, Hedgehog signaling complex consisting of Fu, Cos2, and Ci. The various activities of components are indicated by color (*red*, repressor; *green*, activator), and Ci^{ACT} refers to a highly activated state. Sufu (not depicted) is predicted to be cytosolic by these models.

lates all Ci activity (the one-complex model), and one in which two forms of the complex exist to differentially regulate the repressor and activator functions of Ci (the two-complex model) (42–47).

In the one-complex model, the HSC, which at its most basic is composed of Fu, Cos2, and Ci, is always physically associated with equimolar amounts of Smo (see Fig. 1*A*) (48, 49). In general, this Smo-dependent model is largely based upon the idea that Smo regulates all Ci activity through direct association with the HSC (50–53). Thus, Smo would cycle between three main activity states in an Hh-dependent manner. In the absence of Hh, this Smo-associated complex would function to convert Ci into its repressor form, Ci_{75}, which would presumably occur on endosomes. In the presence of low levels of Hh the processing of Ci into Ci_{75} would be attenuated, leading to an accumulation of full-length Ci, and low level activity. In response to higher levels of Hh, Ci would be converted into a high activity form, and this activation would likely occur on Smo.

The two-complex model argues that there are at least two forms of the HSC: one that is bound to membranes through Smo association and another that is directly associated with membranes in a manner independent of Smo association (Fig. 1*B*) (43). These two forms of the HSC would have different functions; one form converts Ci into a potent transcriptional activator (HSC-A) in response to Hh, while the other form helps convert full-length Ci into its repressor form (HSC-R) in the absence of Hh. Various intermediate states of the HSC-R and HSC-A may also exist to differentially affect Ci stability and activation, depending upon the strength and duration of the Hh signal. Additionally, it is possible that not all of the components are found within these specific complexes and that some proportion exists in other complexes or as free cytosolic proteins as well. The somewhat paradoxical experimental results that culminated in the two-complex model were the observations that Hh stimulation resulted in a translocation of the majority of Cos2 from a vesicular membrane enriched pool to a more cytosolic localization (46), while at the same time the ratio of Cos2-based HSC associated with the transmembrane protein Smo increased (50–52). In order for both of these observations to occur simultaneously, the population of Cos2 associated with Smo would have to be relatively small and the population of Cos2 that relocalizes to the cytosol would have to come from a larger vesicular enriched Cos2 population distinct from that of the pool associated with Smo. Thus, this larger Cos2 population associated with the HSC-R is predicted to be present in greater amounts than the population of Cos2 associated with Smo, the HSC-A, and to bind to vesicular membranes in a Smo-independent fashion. Upon Hh stimulation, three major events might then take place: 1) the HSC-R releases from membranes and

microtubules, 2) proteolysis of Ci is halted, which stabilizes full-length Ci within the HSC-R, and 3) the small pool of Smo-bound HSC-A translocates to the plasma membrane, activating and releasing Ci to the nucleus to promote high level target gene transcription.

One major prediction of the two-complex model is that these various Hh signaling components will not exist in equimolar ratios within cells, with Smo existing in limiting amounts relative to Cos2. Here, we begin to test these predictions by quantifying the molar ratio of the core downstream Hh signaling components. We show that Smo is indeed a limiting component within cells, whose steady-state molar ratio is approximately one-tenth that of Cos2 and Fu. Surprisingly, we also show that Sufu levels are hundreds of times greater than that of Smo and that Sufu's experimental behavior is consistent with it existing in vast molar excess relative to the other components of the HSC. We also present evidence that, despite large differences in the total steady-state ratio of these signaling components, the association of core Hh signaling components within a specific complex is roughly equimolar. Altogether, our quantitation results appear most consistent with the two-complex model of Hh signaling.

EXPERIMENTAL PROCEDURES

Molecular Biology and Cell Culture—Sf21 and S2 cells were cultured in Grace's insect medium (Invitrogen) or Schneider's *Drosophila* medium (Sigma), respectively, which were supplemented with 10% fetal bovine serum and 1% penicillin-streptomycin. Cl8 cells were cultured as previously described (54). Cells were transfected with Cellfectin (Invitrogen) according to the manufacturer's instructions. pActin-Hh has been previously described and was used in various amounts depending on the specific experiment, using empty pAc 5.1a vector (Invitrogen) to normalize the amount of DNA (26). His-SmoN and full-length FLAG-tagged baculoviral expression constructs of Fu, Cos2, and Ci have previously been described (49, 55). pRSET-Sufu was generated by inserting the full-length Sufu cDNA into the pRSET expression vector (Invitrogen), in-frame with an internal 5′ 6x-histidine epitope tag.

Cellular Lysates and Biochemical Analyses—Subcellular fractionation of cells was performed as previously reported (46). Briefly, cells were Dounce homogenized in hypotonic lysis buffer (HLB) (50 mM β-glycerophosphate, 10 mM NaF, 1.5 mM EGTA, 1 mM dithiothreitol, pH 7.6), then centrifuged at 2,000 × *g* for 10 min at 4 °C to generate a low speed supernatant fraction, which was used for all Hh signaling component quantifications. Where appropriate, low speed supernatant fractions were centrifuged at 100,000 × *g* for 30 min at 4 °C. The resulting supernatant (HSS) was separated from the membrane-enriched pellet (HSP), washed by resuspension in 1× volume of HLB supplemented with 150 mM NaCl, and centrifuged again at 100,000 × *g* for 30 min at 4 °C. The washed HSP was resuspended in HLB containing 1% Nonidet P-40. The samples were volume-normalized, resolved by SDS-PAGE, and analyzed by immunoblotting using the following antibodies: rabbit anti-Sufu (49), rat anti-Ci 2A1 (56), mouse anti-Cos2 5D6 (57), rabbit anti-Fu (58), rat anti-SmoC (13), mouse anti-fascicilin1 F5H7, a gift from Dr. M. Hortsch (University of Michigan) (59), and rabbit anti-SmoN, which was generated and purified as previously described (55). Gel-filtration analyses of the various lysates were carried out by using either a Superose 6 or Superose 12 gel-filtration column installed on an AKTA fast-performance liquid chromatography system (Amersham Biosciences), as previously described (48, 60). *Drosophila* embryos were harvested 4–6 h post egg-laying, for maximal Hh pathway activation, and collected as previously described (61–63). Briefly, the collected embryos were washed in 0.7% NaCl, dechorionated, then resuspended in 4 ml of 1% Nonidet P-40 lysis buffer (1% Nonidet P-40, 150 mM NaCl, 50 mM Tris, 50 mM NaF, pH 8.0) per 1 ml of packed embryos and Dounce homogenized. The resulting lysate was centrifuged at 2,000 × *g* for 10 min at 4 °C to separate out cellular debris. Details of embryo collection, as well as details of the gel-filtration analyses and column calibration, can be found in the supplemental "Experimental Procedures." Proteins were immunoprecipitated from *Drosophila* cell lysate essentially as previously described (26). Cl8 hypotonic lysates were fractionated into cytosolic or membrane-enriched fractions and supplemented to a final concentration of 1% Nonidet P-40 prior to use as the immunoprecipitation starting material. Immunoprecipitations were performed using mouse anti-Sufu 25H3 (52) (Developmental Studies Hybridoma Bank) or mouse IgG (Sigma). Complexes were analyzed by SDS-PAGE and immunoblotting as previously described (48).

Purification and Staining of Components for Quantification Standards—All construction and preparation of the FLAG-Fu, FLAG-Cos2, and FLAG-Ci baculoviruses, as well as infections of Sf21 cells and purification steps were done as previously described (49, 57, 64). The 6x-histidine tagged N-terminal Smo peptide (amino acids 48–245) used as a quantification standard was generated as previously described (55). We chose to use this N-terminal fragment of Smo for its ease of purification and handling, as in our hands recombinant Smo appears to aggregate, making analysis and subsequent purification difficult. His-SmoN and His-Sufu were purified, from BL21(DE3)pLysS *Escherichia coli* (Protein Express Inc.), under denaturing conditions using nickel-nitrilotriacetic acid-agarose beads (Qiagen) following the manufacturer's instructions.

Protein staining using Coomassie or silver was performed as previously described (65, 66). Coomassie and silver staining gave comparable protein concentration values for all purified recombinant proteins, with the exception of Sufu. Thus, a third staining method, SYPRO Ruby (Molecular Probes) protein stain, was used following manufacturer's instructions to validate the Sufu concentration. Stained proteins were imaged directly by scanning on an HP Scanjet 8200 or visualized on a Storm PhosphorImager (Amersham Biosciences). The relative density of individual protein bands and signal linearity were determined by using ImageQuant software.

Quantification of the Levels of Endogenous Hh Signaling Components—All components, except Smo, were quantified as described in the text, using full-length recombinant proteins as standards to quantify endogenous levels. Endogenous Smo was quantified using a purified N-terminal Smo peptide as the standard (described in Ref. 55). Calculations to determine the concentration of this smaller recombinant SmoN pep-

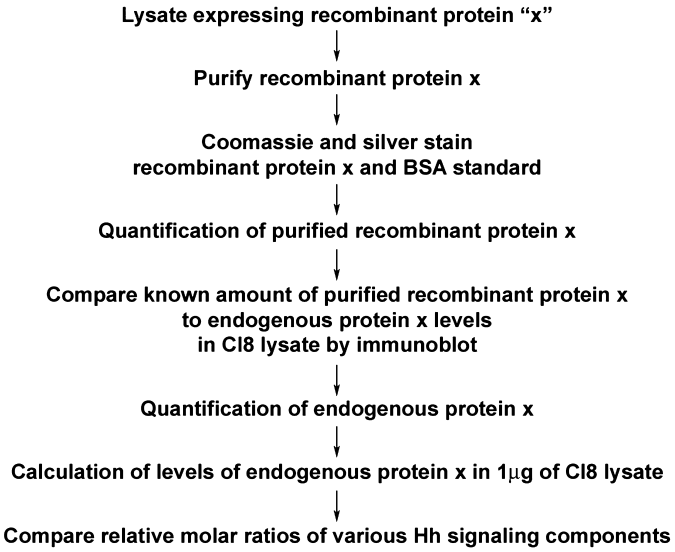

FIGURE 2. **Schematic of quantification method.** Flowchart of method used to quantify Hh signaling components. "*x*" represents any of the core Hh-signaling proteins that were quantified.

tide were converted from nanograms to moles, to account for the difference in molecular weight between this peptide and endogenous Smo. Moreover, to compare these two proteins of different molecular weights, we also had to account for differences in their transfer efficiency during immunoblotting. These transfer efficiency differences were factored into our calculations, although the net change was negligible. Details of these calculations can be found in the supplemental "Experimental Procedures."

A control immunoblot containing 6x-histidine peptides (Covance), in a 100-fold molar excess, was included when using the affinity purified SmoN or Sufu antibodies. This His_6 peptide was included to verify that any immunoblot signal we obtained was not due to contaminating antibodies that recognize the His_6 epitope present on the original antigen. The signals generated by these antibodies were quantified in the presence and absence of this His_6 peptide, and no significant differences were observed.

RESULTS

Quantitation of Core Hh Signaling Components in Cl8 Lysates—To identify the stoichiometric ratio of the key Hh signaling components, we set out to develop a quantitative immunoblotting method for each of these core proteins (Fig. 2). This methodology was developed using the various purified recombinant signaling proteins as standards, which we purified from a baculoviral/Sf21 expression system or from an inducible expression system in *E. coli*. Sf21 cells were infected with baculovirus encoding FLAG-Ci, FLAG-Cos2, or FLAG-Fu, and the respective tagged protein was purified from the lysates of these cells using anti-FLAG immunoaffinity columns (supplemental Fig. S1*a–c*). His-Sufu and a fragment of His-Smo were expressed in bacteria engineered to overexpress each of them, respectively, and purified from the lysates of these cells using nickel-nitrilotriacetic acid affinity columns (supplemental Fig. S1*d* and data not shown).

To use this set of purified recombinant proteins as quantitative immunoblotting standards, it was first necessary to determine the concentration of each purified protein. This quantification methodology was repeated for each core component. Data for Sufu are shown here (Fig. 3), and data for Ci (supplemental Fig. S2), Cos2 (supplemental Fig. S3), Fu (supplemental Fig. S4), and Smo (supplemental Fig. S5), are presented in the supplemental materials. Aliquots of purified recombinant Sufu were compared with increasing amounts of pure bovine serum albumin (BSA) on a series of SDS-polyacrylamide gels, then analyzed using various protein stains (Fig. 3, *A* and *B*, and Table 1). The density of the protein staining for both the increasing amounts of BSA and purified recombinant Sufu was determined with ImageQuant software. Each amount of BSA was plotted against its corresponding density value to generate an equation describing this correlation. The relative density values for the purified recombinant Sufu were substituted into this equation to obtain the relative amount of recombinant Sufu present in a specific volume. The values for each experimental repeat and for each protein staining method were then averaged together to yield a single concentration value. Quantitating the purified recombinant protein standards in this manner allowed us to determine only the protein concentration of the correct molecular weight. This negated the contribution of any contaminating proteins to the concentration of each purified recombinant protein preparation.

To determine the quantity of each key component of the Hh-signaling pathway in a cell, we compared known concentrations of the purified recombinant protein to the amount of the endogenous component in a set amount of lysate from the *Drosophila* Clone-8 (Cl8) imaginal disc cell line, which possesses an intact Hh-signaling pathway, via immunoblotting (Fig. 3*C*) (67). This comparison allowed us to generate an equation, which was subsequently used to determine the amount of the specific endogenous component. This number was further converted into moles of endogenous protein per 1 μg of Cl8 protein (Table 1), for ease of comparison between the various components. Using the values determined with these purified signaling protein standards, we calculated that there are $\sim 94 \times 10^{-16}$ mol of Sufu, 10×10^{-16} mol of Fu, 4×10^{-16} mol of Cos2, 2×10^{-16} mol of full-length Ci, and 3×10^{-17} mol of Smo, in 1 μg of Cl8 protein (Table 1). Therefore, the steady-state molar ratio of Sufu to Fu to Cos2 to Ci to Smo in Cl8 cells is 312:34:12:6:1. Upon addition of Hh, only Ci and Smo levels changed, increasing ~5-fold and 2-fold, respectively (supplemental Fig. S6 and Table 1). The two-complex model does not require a 1:1 Cos2 to Smo ratio, as the one-complex model does, indicating that the ratio that we have determined is more consistent with the two-complex model of Hh signaling.

Quantitation of Hh Signaling Components in S2 Cells and Drosophila Embryos—To determine whether the ratio of core signaling components observed in Cl8 cells was comparable in different cell types, we quantified the same core components in both S2 cells, a cell line derived from *Drosophila* embryos, and *Drosophila* embryo extracts (68). We prepared protein normalized cell extracts of Cl8 and S2 cells and compared them by immunoblotting (Fig. 4*A*). Comparison of the levels of each component revealed an overall similar ratio of components in

S2 cells as in Cl8 cells (Table 2), with the exception of Ci, which is not expressed in S2 cells (28). Sufu levels remained in excess, while Smo levels remained limiting. However, quantification of the relative levels of components over many independent replicates showed that Cos2 levels were statistically increased ($p \leq 0.05$) over that observed in Cl8 cells (Fig. 4*B*). The reason for this increase is unknown, but it is possible that the absence of Ci in these cells somehow affects the stabilization of Cos2. Extracts from *Drosophila* embryos also showed similar levels of all core components relative to Cl8 cells (Fig. 4*C* and Table 2). We anticipated that the embryo extracts would consist of cells that were exposed to various levels of Hh, which might result in

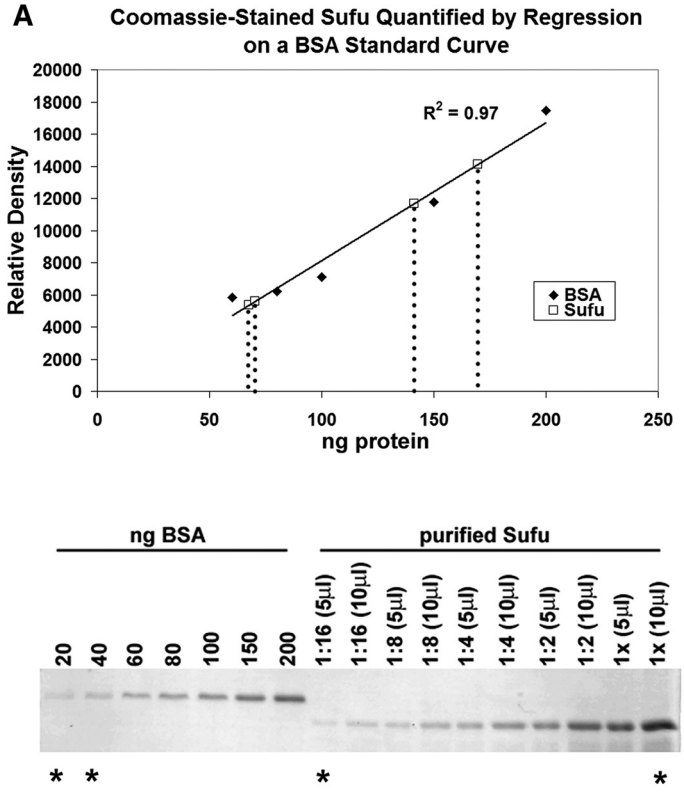

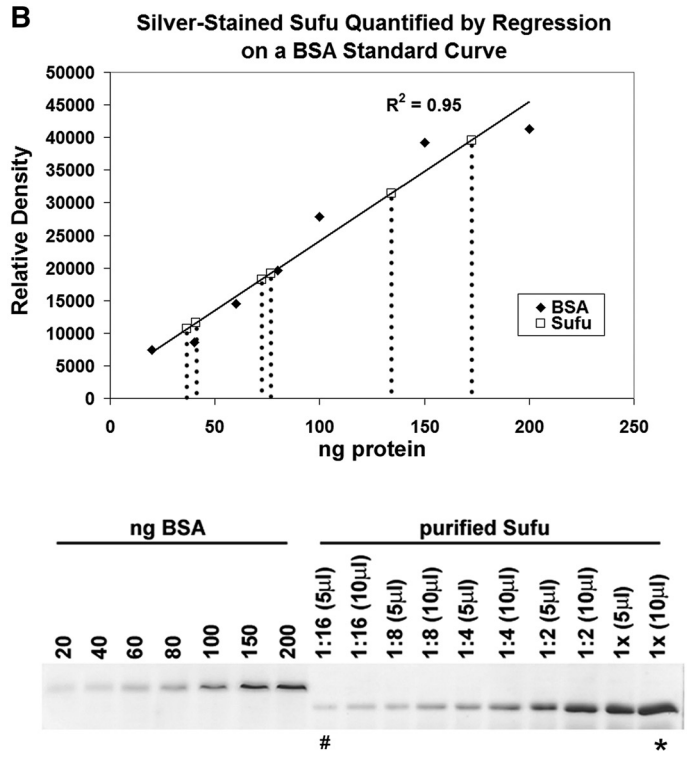

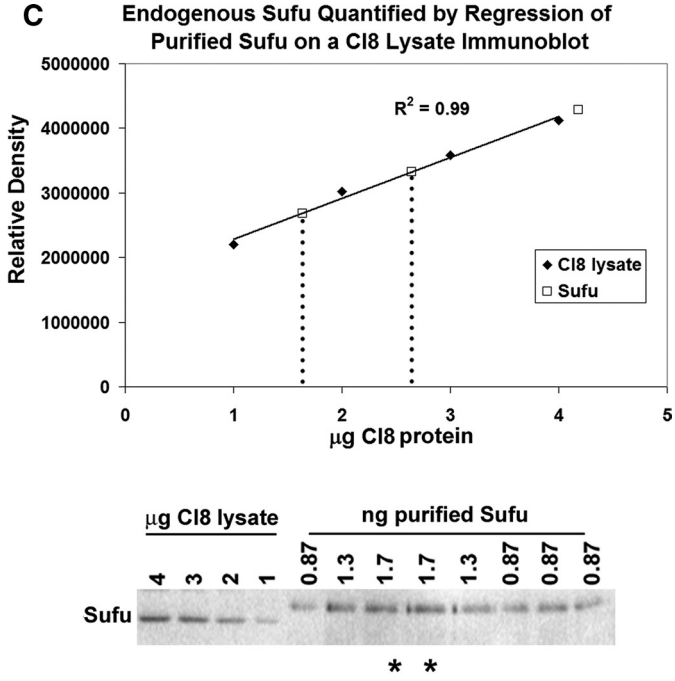

TABLE 1

Summary of Hh signaling component quantification in Cl8 cells

Table I summarizes the quantification process and outcome for each of the Hh signaling components. The "Tag" column indicates how the component was epitope tagged for purification. The "Methods of Quantification" column indicates which protein staining methods were used to determine the average concentration (ng/μl) of the purified sample, which is shown in the adjacent column. These purified component proteins were then used as standards to quantify the number of moles of their corresponding endogenous protein in 1 μg of Cl8 protein. The "Ratio" column translates the number of moles per μg of each component into a ratio that is normalized to 1 mol of Smo. The relative amount of some components appears to be modulated in response to Hh, indicated in the "Ratio +Hh" column. We quantitated the various changes in protein component levels we observed in Cl8 cells (supplemental Fig. S6).

Component	Tag	Methods of quantification (against BSA standard)	Average conc. of pure standard	Cl8 lysate	Ratio	Ratio (+Hh)
			ng/μl	*mol/μg*		
Smo	His	Silver, Coomassie	73.9	3.0×10^{-17}	1	2-fold increase
Ci	FLAG	Silver, Coomassie	3.6	1.80×10^{-16}	6	5-fold increase
Cos2	FLAG	Silver, Coomassie	3.0	3.60×10^{-16}	12	No change
Fu	FLAG	Silver, Coomassie	5.0	1.02×10^{-15}	34	No change
Sufu	His	Silver, Coomassie, SYPRO Ruby	115.3	9.40×10^{-15}	312	No change

elevated levels of Smo and Ci (1, 28, 55). Consistent with this expectation, Smo and Ci levels in *Drosophila* embryo lysate exhibited a statistically significantly increase ($p \leq 0.05$) relative to Cl8 cells, when compared over many independent replicates (Fig. 4*D*). The ratio of the signaling components relative to Cl8 cells, as well as the absolute ratio of components, in which total levels are normalized to the most limiting component, is summarized in Table 2. In short, a similar ratio of signaling components was observed from lysates of two *Drosophila* cell lines and from the lysate of a physiologically relevant tissue. The conservation of this ratio *in vivo* indicates the biological relevance of the relative levels of these components.

Biochemical Characterization of Core Components Validates Observed Ratios—The development of the two-complex model was based upon results obtained from S2 cells, which lack Ci, and *Drosophila* embryo extracts, which contain a mixture of cells exposed to varying levels of Hh (1, 28). To begin to validate the ratio of components that we observed in Cl8 cells and embryo extracts, we investigated the localization of these components in Cl8 cells. We separated Cl8 lysates into two crude fractions; a membrane-enriched fraction and a cytosolic fraction. In the absence of Hh, the bulk of Cos2 and Fu, along with approximately half of the total Ci, are found in the membrane-enriched fraction (Fig. 5*A*). Upon addition of Hh, Ci is stabilized and the majority of these HSC components enrich in the cytosolic fraction, consistent with results previously obtained with S2 cells (46). However, Sufu appears to differentially localize relative to the other HSC components, enriching in the cytosolic fraction in both the presence and absence of Hh. These results, along with our quantitation of Sufu, might indicate that the vast majority of Sufu is not associated with Fu, Cos2, and Ci. In addition, size-exclusion chromatography showed that the bulk of the cytosolic Sufu migrates between the 66 and 43 kDa molecular mass markers (Fig. 5*B*), consistent with Sufu, a 54-kDa protein, existing in the cytosol as a monomer. These results suggest that the majority of Sufu is not bound to the other HSC members and appears to exist as a cytosolic enriched, monomeric protein.

Although we show that the majority of Sufu likely exists as a cytosolic enriched monomer, Sufu has been previously shown to associate with both Ci and Fu (32, 33, 49, 69). We hypothesized, based on our quantitation results, that these somewhat opposing findings might be the result of the large molar excess of Sufu relative to the other components of the HSC. As the vast majority of Sufu is cytosolic, we further speculated that a small population of Sufu enriching with the HSC might be more easily visualized from membrane-enriched lysates. Additionally, we have previously demonstrated that the biologically relevant pool of Fu, Cos2, and Ci is found in a membrane-bound complex, further indicating that a potential pool of Sufu relevant to Hh signaling might be found in association with membranes (48). Therefore, we fractionated Cl8 extracts into membrane- or cytosol-enriched fractions and subjected each pool to immunoprecipitation with antibodies to Sufu or nonspecific IgG (Fig. 6*A*). A large amount of Sufu was immunoprecipitated from the cytosolic-enriched fraction, along with some associated Ci. Consistent with our speculation, a small population of Sufu was also immunoprecipitated from the membrane-enriched fraction. Interestingly, this smaller population of Sufu associates with a greater percentage of Ci than the cytosolic population of Sufu. These results suggest that there is a membrane-localized population of Sufu, which represents a minority of Sufu, and that this population may be responsible for the bulk of its association with the HSC. This small pool of Sufu

FIGURE 3. **Quantification of endogenous Sufu levels in Cl8 cell lysates.** *A*, purified recombinant Sufu was quantified by Coomassie staining various dilutions of the purified sample alongside increasing amounts of BSA, which had been separated by SDS-PAGE (*bottom panel*). The signal intensity of BSA and purified recombinant Sufu were quantitated by ImageQuant software. The *top panel* shows the results of this quantitation, with each different amount of BSA plotted against its corresponding density. These BSA density values (◆) were used to generate an equation ($y = 90x - 440$, $R^2 = 0.97$), from which the concentration of pure recombinant Sufu was calculated. The calculated amounts of Sufu were then also plotted on the line (□). *B*, purified recombinant Sufu was quantified by silver staining in the same manner as described for Coomassie staining in *A*. BSA density values (◆) were used to generate an equation ($y = 200x + 2850$, $R^2 = 0.95$), from which the concentration of pure recombinant Sufu was calculated and plotted on the line (□). *C*, endogenous levels of Sufu in Cl8 lysate were quantified by comparison to known amounts of purified recombinant Sufu by immunoblotting, and graphically represented in the *top panel*. A standard curve of Cl8 lysate, which was run in duplicate and the averaged points plotted, was used to generate an equation ($y = 631{,}000x + 1{,}650{,}000$, $R^2 = 0.99$), to which known amounts of purified recombinant Sufu were compared with determine the amount of Sufu present in 1 μg of Cl8 protein. The amount of endogenous Sufu was calculated to be 9.4×10^{-15} mol of Sufu per 1 μg of Cl8 protein. A representative immunoblot showing the endogenous Sufu signal (*left*) adjacent to the purified recombinant Sufu signal (*right*) is shown in the *lower panel*. In all *panels* shown, an *asterisk* represents a point that was excluded from our analyses, because it either did not fall within the standard curve or within the detection range of the ImageQuant software. All points of duplicate concentrations were averaged and plotted as a single point. A pound sign (#) indicates that the point was plotted as an individual value, because a duplicate was not available.

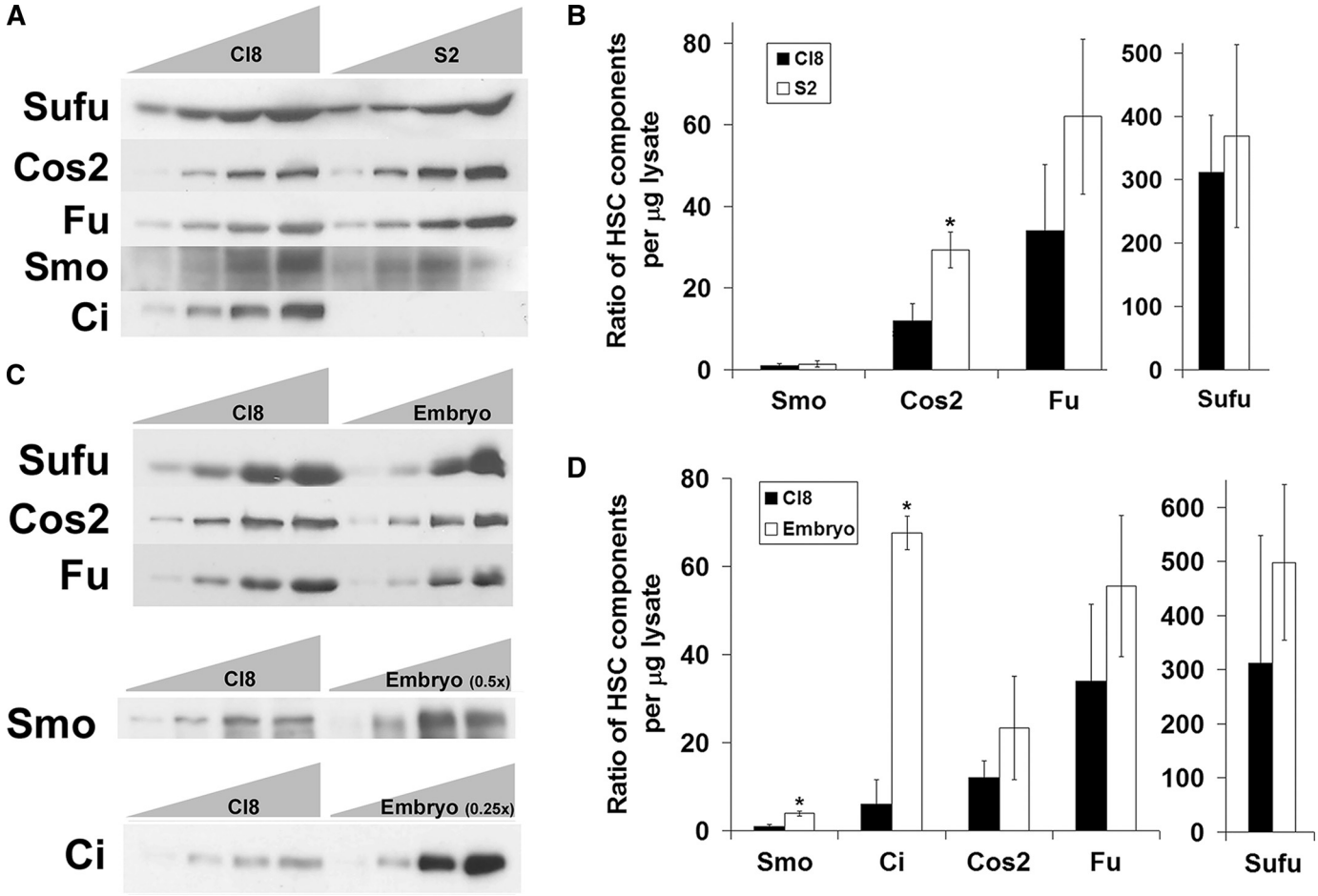

FIGURE 4. **Comparison of Hh signaling components between *Drosophila* cell lines and *Drosophila* embryos.** *A*, representative immunoblots showing increasing amounts of Cl8 lysate alongside increasing amounts of S2 cell lysate allow a comparison of the ratio of components present in each. Samples were normalized to protein concentration and increasing volumes of lysates (indicated by *gray triangles above*), were separated by SDS-PAGE and immunoblotted with antibodies to the indicated Hh signaling component. *B*, quantitation of the relative levels of each component present in 1 μg (μg) of Cl8 or S2 lysate using ImageQuant software. Sufu is shown on a separate scale, to show differences in the less abundant components (*right panel*). The relative ratios of components are shown in Table 2. *C*, representative immunoblots showing increasing amounts of Cl8 lysate alongside increasing amounts of *Drosophila* embryo lysate allow a comparison of the ratio of components present in each. Samples were normalized to protein concentration, and increasing volumes of lysate (indicated by *gray triangles above*) were loaded as undiluted samples or dilutions (as indicated by 0.5× or 0.25×). *D*, quantitation of the relative levels of each component present in 1 μg of Cl8 or embryo lysate using ImageQuant software. Sufu is shown on a separate scale, to show differences in the less abundant components (*right panel*). The *asterisk* indicates the relative level of that component in S2s or embryos is significantly different ($p \leq 0.05$) in comparison to Cl8s, as calculated by a Student's *t* test (two-tailed). Standard deviation is indicated by *error bars*, and a minimum of three replicates per component was used for all calculations.

TABLE 2

Summary of Hh signaling component quantification in S2 cells and *Drosophila* embryos

This table summarizes the relative ratio of components present in Cl8 cells, S2 cells, and embryo extracts, as determined in Fig. 4. The columns labeled "Ratios relative to Cl8s" represent the steady-state concentration of components within S2 cells or embryos, normalized to the calculated ratio of these components in Cl8 cells. The columns labeled "Absolute ratios" represent the steady-state concentration of components within S2 cells or embryos, with each component normalized to the most limiting component.

Component	Ratio in Cl8s	Ratios relative to Cl8s		Absolute ratios	
		S2s	Embryos	S2s	Embryos
Smo	1	1.4	4	1	1
Ci	6	0	68	0	17
Cos2	12	30	23	21	6
Fu	34	62	55	44	14
Sufu	312	369	496	263	124

is likely a biologically relevant fraction, which binds Ci to negatively regulate its activity from within the membrane-associated HSC, while the larger cytosolic pool of Sufu may serve to bind any freely diffusible Ci in the cytosol, providing multiple layers of regulation.

When subjected to fractionation by gel filtration, Fu can be observed in three separate populations, termed A, B, and C (48). Populations A and B are much larger than the molecular size of Fu itself, ~40,000 and 700 kDa, respectively, and signify the involvement of Fu in high molecular weight HSCs (48). Immunoprecipitation of Fu from population B showed Fu binding to Cos2, whereas immunoprecipitation from population A showed Fu associating with both Ci and Cos2 (48). Thus, population A was proposed to be the biologically relevant fraction, because it contains Ci and is enriched on cell membranes (46, 48). Consistent with this proposal, when salt-extracted proteins from a Cl8 membrane-enriched pellet were fractionated on a Superose 6 gel-filtration column, Fu, Cos2, and Ci appear to co-elute in a large molecular sized peak similar to population A (Fig. 6*B*). Because Smo is a transmembrane protein, it is not extracted by this method

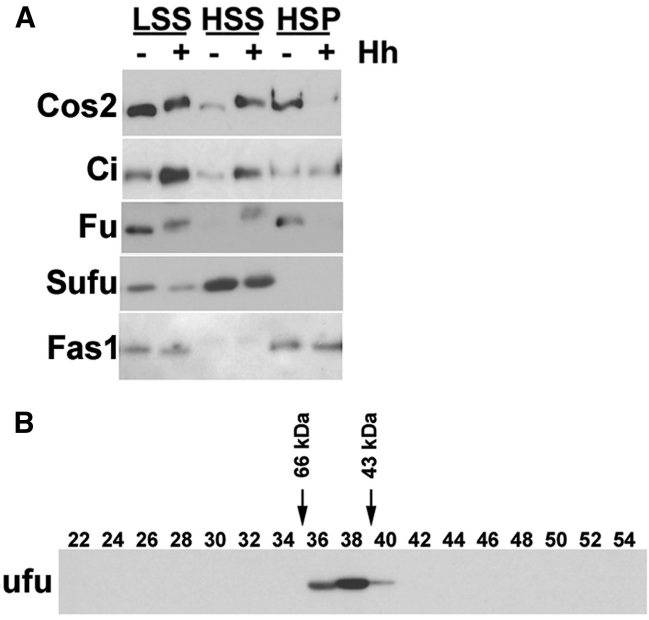

FIGURE 5. **The bulk of Sufu does not associate with the HSC.** *A*, subcellular fractionation of Cl8 lysate shows differential localization of HSC components in the presence (+) and absence (−) of Hh. In the absence of Hh, Cos2 and Fu, as well as a portion the total Ci, are primarily found in the membrane-enriched fraction (HSP), whereas Sufu is localized primarily in the cytosol. In the presence of Hh, the bulk of these proteins are found in the cytosolic enriched fraction (HSS). Fasciclin1 (*Fas1*) is a marker of the membrane-enriched fractions, which was also used to validate protein normalization. *B*, fractionation of the cytosolic enriched HSS on a Superose 12 gel-filtration column shows that Sufu migrates in a manner consistent with it being primarily monomeric. An immunoblot of the even-numbered trichloroacetic acid-precipitated fractions is shown here. The migration of two known protein standards is indicated above the immunoblot.

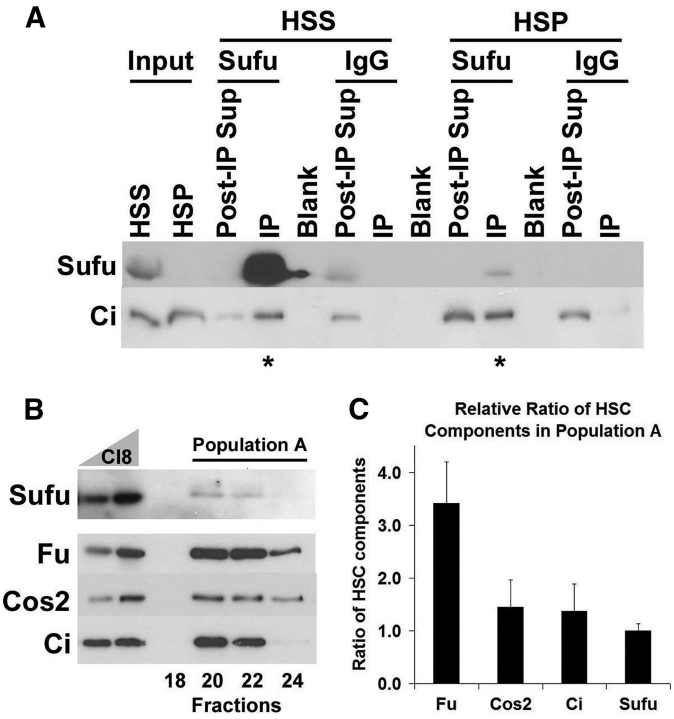

FIGURE 6. **A minor population of membrane-localized Sufu associates with the HSC.** *A*, Sufu association with Ci is increased in a membrane-enriched fraction. *Input lanes* indicate the starting material and the "*Post-IP Sup*" lanes indicate the post-immunoprecipitation supernatant, which contains proteins that were not bound by the antibody-bead complexes. A large amount of Sufu is immunoprecipitated from the HSS and is able to co-precipitate Ci. A small amount of Sufu is immunoprecipitated from the HSP, but is able to co-precipitate a similar amount of Ci, indicating that membrane-associated Sufu binds a greater proportion of the total Ci (compare lanes marked by an *asterisk*). IgG lanes serve as a control and indicate that immunoprecipitation of Sufu and Ci is specific to the antibody used. *B*, a small population of Sufu co-migrates with other HSC members from a membrane-enriched fraction. Membrane-associated proteins were extracted from HSP fractions with 0.5 M NaCl and fractionated over a Superose 6 gel-filtration column. The various *even-numbered fractions* were trichloroacetic acid-precipitated and immunoblotted using the appropriate antibodies. A peak containing Fu, Ci, Cos2, and Sufu is seen in *fraction 22*, where the previously described population A migrates. Undiluted Cl8 lysate is shown as a standard in Fu, Cos2, and Ci immunoblots. Cl8 lysate diluted to 1/10th of its original concentration is shown as a standard in the Sufu immunoblot (*top panel*), due to Sufu's higher concentration. *C*, quantification of the relative ratio of the components observed in population A, shows ~2 mol of Fu, 1 mol of Cos2, 1 mol of Ci, and 1 mol of Sufu. Immunoblot signals in *fraction 22* were quantified with ImageQuant software using Cl8 lysate as a standard ($n = 3$). Standard deviation is indicated by *error bars*.

and thus would not appear in this fraction (9, 10). Interestingly, Sufu also appeared to co-migrate in this population (Fig. 6*B*, *uppermost panel*). Because the vast majority of Sufu is found in the cytosol (Fig. 5), the membrane-localized pool of Sufu shown here is relatively small in comparison. Known amounts of Cl8 protein were used as a standard to quantitate the relative ratio of the HSC components in this peak of population A (Fig. 6*B*). The ratio of these co-migrating components is approximately equal to 2 molecules of Fu and 1 molecule each of Cos2, Ci, and Sufu (Fig. 6*C*). It is possible that population A migrates at a higher molecular weight due to the association of other accessory proteins or as a consequence of its physical size and shape, because shape can affect the migration of proteins through a gel-filtration column. Alternatively, the large molecular size of population A may indicate that several copies of each protein are present, while maintaining the same overall ratio. Thus, although the ratio of Hh signaling components may span more than two orders of magnitude within cells, the molar ratio may be quite similar for the core components within these multicomponent protein complexes. The relatively equimolar association of these four signaling components implies a biologically relevant relationship within this membrane-associated complex.

DISCUSSION

Current models of Hh signaling account for a wide variety of genetic and biochemical information, while at the same time condensing complex results into simple testable hypotheses (42–47). One essential piece of information that all of the current models omit is the relative molar ratio of Hh-signaling components in cells. Here, we have determined the endogenous, steady-state concentration of the five core components of Hh signaling. We have demonstrated that Smo is present in limiting amounts relative to Cos2, which is consistent with the previously proposed two-complex model of Hh signaling (42, 43, 46). These results are consistent between two *Drosophila* cell lines and in *Drosophila* embryos, a physiologically relevant tissue. Interestingly, we noted that Sufu exists in vast molar excess to the other HSC components. We provided evidence for two separate populations of Sufu, showing that the majority of Sufu is localized in the cytosol and appears to be monomeric, while a second smaller population of Sufu associates with the HSC on cellular membranes. As such, these Sufu results are consistent with it

being in large molar excess relative to the other HSC components, validating our quantification results.

The major mechanistic difference between the one-complex and two-complex models is that the latter model assumes that the conversion of Ci into its most active forms occurs within a dedicated HSC, the HSC-A, which is distinct from the bulk of the HSC, the HSC-R (42, 43, 46). The one-complex model emphasizes various activation states in which Smo may exist (44, 45, 47), whereas the two-complex model emphasizes various activation states in which the HSCs may exist (42, 43, 46). The one-complex model assumes equimolar ratios of Smo and Cos2, whereas the two-complex model assumes that Cos2 is in stoichiometric excess to Smo. In the latter scenario, the bulk of Cos2 is found in the HSC-R and is not associated with Smo (46). The simplest test of these models requires us to know the relative ratio of these signaling components. Our quantitative analyses reveal a ratio of Hh-signaling components that is most consistent with the two-complex model, because Cos2 is present in 10-fold molar excess to Smo. The one-complex model requires a different ratio of components, as it predicts that Cos2 binds to membranes solely via Smo. In order for our data to support the one-complex model, each molecule of Smo present in cells would have to associate with twelve molecules of Cos2 at any given time. However, if one assumes that one molecule of Smo can only bind to a single Cos2-scaffolded HSC, ~90% of the remaining HSC would likely be found associated with vesicular membranes in a Smo-independent fashion, which is consistent with the two-complex model and our earlier work (42, 46). Even in the presence of Hh, which increases Smo levels ~2-fold (supplemental Fig. S6), the amount of Smo present within a cell would be insufficient to bind to the majority of Cos2 present (supplemental Fig. S6*a* and Table 1). However, if Cos2 becomes degraded in response to Hh, as has been suggested, a larger percentage of the remaining Cos2 would be associated with Smo, as has been observed by indirect immunofluorescence microscopy (50).

The approach we have taken to quantitate the components of the Hh-signaling pathway has been used by many laboratories to quantitate the relative components of numerous biological processes (70–72). Even so, such an approach makes a number of assumptions that may bias the interpretations of the results presented here. For example, it assumes that the protein-staining method used does not differentially stain the various recombinant Hh-signaling proteins relative to a BSA standard. Because each protein stain produces a visible signal dependent on a different spectrum of amino acids (73), we utilized two different protein-staining methods to minimize any effects such differential staining might have on the estimation of the relative abundance of the endogenous signaling proteins. Furthermore, if the protein concentrations obtained with these two distinct methods were not within 25% percent of each other we employed a third protein-staining method, and then calculated a numerical average of the three methods. Our quantification methodology also assumes that similar levels of detection are obtained between the various recombinant protein standards and their endogenous counterparts. However, a number of these endogenous proteins are known to be post-translationally modified in ways that alter their migration upon SDS-PAGE. To reduce any such underestimates of endogenous components, we used SDS-polyacrylamide gels containing a high percentage of acrylamide to collapse slower migrating isoforms into a single band. We then used ImageQuant software to outline and quantitate multiple isoforms of the various endogenous proteins, if they were still observed. Even with these precautions it remains possible that post-translational modification of the endogenous proteins might impact their relative quantitation. However, such a possibility might be true regardless of the available methodology used for such quantitation.

As Smo is required for all aspects of Hh signaling, it must communicate with the entire pool of HSC regardless of how many of these pools exist (9, 10). Two mechanisms by which a limiting amount of one signaling component, such as Smo, can regulate a much larger pool of downstream signaling proteins are through the activation of intermediate signal amplifying molecules, or through the limiting component cycling through the larger pool of downstream signaling proteins in a dynamic manner (74, 75). We have recently provided evidence for the existence of both mechanisms in Hh signaling (13, 26). We found that 1) Smo regulates the common second messenger cAMP, through activation of the heterotrimeric guanine nucleotide binding protein $G\alpha_i$, and 2) Cos2 functions as a kinesin-related protein to regulate the dynamic microtubule-based movement of the HSC (13, 26). Combined, these results suggest that the HSCs might associate with Smo in a dynamic recycling model, in a manner that combines various aspects of the one-complex and two-complex models. Under these conditions, the response of the HSC would be dictated by the Smo activity state, with Cos2 moving the various HSCs to and from Smo. This is also consistent with our observation that the bulk of the HSC is not directly associated with Smo under steady-state conditions (46). Therefore, we propose that Smo regulates HSC-A and HSC-R, and does so in a manner that requires both direct and indirect interactions with Smo (13, 26, 42). Thus, the two populations of HSC, HSC-A and HSC-R, would act as dynamic multiprotein complexes, whose flux is ultimately regulated by Cos2 motility.

Quantitation of the HSC components also revealed that the levels of Sufu, in the absence of Hh, are more than 300 × that of Smo. This unexpected finding is consistent with our biochemical characterization of Sufu, which shows that the predominant form of Sufu is monomeric and not associated with the HSC. However, we also provide evidence for a much smaller population of Sufu, which is in a membrane-associated complex with Cos2, Fu, and Ci. The amount of Sufu binding to the membrane-associated HSC appears to be equimolar to the other components, despite its vast molar excess relative to the other HSC components. It is not clear what role, if any, the larger cytoplasmic pool of Sufu plays in Hh signaling. This latter population of Sufu may also function in other signal transduction pathways, with distinct pools of Sufu localizing to various scaffolding proteins that render it specific for that particular signaling pathway (76, 77). These additional proposed roles of Sufu would have to exist in a redundant fashion with other such proteins, given the weak phenotype of *Drosophila* lacking *Sufu*

function (31, 35, 78). It is also possible that in the absence of Hh this large cytoplasmic pool of Sufu functions to buffer any free cytoplasmic Ci into an inactive state. This latter speculation would certainly be consistent with the genetics of *Sufu*, which appears to regulate Hh signaling in a dose-dependent fashion in a sensitized background (35, 78–80).

Quantitative analysis and modeling of signaling pathways can reveal important information about the dynamics of a system, including rate-limiting steps, flux, and affinities (81). For example, recent quantitation of the Wnt signaling pathway identified low levels of axin as a rate-determining step in this signaling pathway, providing new insight into fluctuations in the amplitude of β-catenin response (81). Our quantitation of the core Hh signaling components is the first step toward developing such dynamic models of the Hh pathway. Such models will not only expand our mechanistic insight into how signal transduction pathways operate within cells, but may also translate into the rational drug design of small-molecules that only inhibit specific arms of the Hh-signaling pathway.

Acknowledgments—We thank Drs. Anne Plessis (Institut Jacques Monod), Joan Hooper (University of Colorado, Boulder), Yashi Ahmed (Dartmouth), and Ethan Lee (Vanderbilt University) for helpful discussions throughout this work. We also thank Dr. Thomas Kornberg for the serum from which the SmoN antibody was purified and Dr. Scott Gerber for his expert advice and help with manuscript revisions. The Sufu (25H3) antibody used here was obtained from the Developmental Studies Hybridoma Bank developed under the auspices of the NICHD, National Institutes of Health and maintained by the University of Iowa.

REFERENCES

1. Ingham, P. W., and McMahon, A. P. (2001) *Genes Dev.* **15,** 3059–3087
2. Torroja, C., Gorfinkiel, N., and Guerrero, I. (2005) *J. Neurobiol.* **64,** 334–356
3. McMahon, A. P., Ingham, P. W., and Tabin, C. J. (2003) *Curr. Top. Dev. Biol.* **53,** 1–114
4. Rubin, L. L., and De Sauvage, F. J. (2006) **5,** 1026–1033
5. Robbins, D. J., and Hebrok, M. (2007) *EMBO Rep.* **8,** 451–455
6. Hooper, J. E., and Scott, M. P. (1989) *Cell* **59,** 751–765
7. Chen, Y., and Struhl, G. (1996) *Cell* **87,** 553–563
8. Chen, Y., and Struhl, G. (1998) *Development* **125,** 4943–4948
9. Alcedo, J., Ayzenzon, M., Von Ohlen, T., Noll, M., and Hooper, J. E. (1996) *Cell* **86,** 221–232
10. van den Heuvel, M., and Ingham, P. W. (1996) *Nature* **382,** 547–551
11. Marigo, V., Davey, R. A., Zuo, Y., Cunningham, J. M., and Tabin, C. J. (1996) *Nature* **384,** 176–179
12. Stone, D. M., Hynes, M., Armanini, M., Swanson, T. A., Gu, Q., Johnson, R. L., Scott, M. P., Pennica, D., Goddard, A., Phillips, H., Noll, M., Hooper, J. E., de Sauvage, F., and Rosenthal, A. (1996) *Nature* **384,** 129–134
13. Ogden, S. K., Fei, D. L., Schilling, N. S., Ahmed, Y. F., Hwa, J., and Robbins, D. J. (2008) *Nature* **456,** 967–970
14. Nakano, Y., Nystedt, S., Shivdasani, A. A., Strutt, H., Thomas, C., and Ingham, P. W. (2004) *Mech. Dev.* **121,** 507–518
15. Ingham, P. W., Nystedt, S., Nakano, Y., Brown, W., Stark, D., van den Heuvel, M., and Taylor, A. M. (2000) *Curr. Biol.* **10,** 1315–1318
16. Denef, N., Neubüser, D., Perez, L., and Cohen, S. M. (2000) *Cell* **102,** 521–531
17. Martín, V., Carrillo, G., Torroja, C., and Guerrero, I. (2001) *Curr. Biol.* **11,** 601–607
18. Strutt, H., Thomas, C., Nakano, Y., Stark, D., Neave, B., Taylor, A. M., and Ingham, P. W. (2001) *Curr. Biol.* **11,** 608–613
19. Hooper, J. E. (2003) *Development* **130,** 3951–3963
20. Zhao, Y., Tong, C., and Jiang, J. (2007) *Nature* **450,** 252–258
21. Sisson, J. C., Ho, K. S., Suyama, K., and Scott, M. P. (1997) *Cell* **90,** 235–245
22. Alves, G., Limbourg-Bouchon, B., Tricoire, H., Brissard-Zahraoui, J., Lamour-Isnard, C., and Busson, D. (1998) *Mech. Dev.* **78,** 17–31
23. Orenic, T. V., Slusarski, D. C., Kroll, K. L., and Holmgren, R. A. (1990) *Genes Dev.* **4,** 1053–1067
24. Forbes, A. J., Nakano, Y., Taylor, A. M., and Ingham, P. W. (1993) *Dev. Suppl.* 115–124
25. Von Ohlen, T., Lessing, D., Nusse, R., and Hooper, J. E. (1997) *Proc. Natl. Acad. Sci. U.S.A.* **94,** 2404–2409
26. Farzan, S. F., Ascano, M., Jr., Ogden, S. K., Sanial, M., Brigui, A., Plessis, A., and Robbins, D. J. (2008) *Curr. Biol.* **18,** 1215–1220
27. Ho, K. S., Suyama, K., Fish, M., and Scott, M. P. (2005) *Development* **132,** 1401–1412
28. Aza-Blanc, P., Ramírez-Weber, F. A., Laget, M. P., Schwartz, C., and Kornberg, T. B. (1997) *Cell* **89,** 1043–1053
29. Wang, Q. T., and Holmgren, R. A. (1999) *Development* **126,** 5097–5106
30. Alexandre, C., Jacinto, A., and Ingham, P. W. (1996) *Genes Dev.* **10,** 2003–2013
31. Ohlmeyer, J. T., and Kalderon, D. (1998) *Nature* **396,** 749–753
32. Méthot, N., and Basler, K. (2000) *Development* **127,** 4001–4010
33. Wang, G., Amanai, K., Wang, B., and Jiang, J. (2000) *Genes Dev.* **14,** 2893–2905
34. Smelkinson, M. G., Zhou, Q., and Kalderon, D. (2007) *Dev. Cell* **13,** 481–495
35. Préat, T. (1992) *Genetics* **132,** 725–736
36. Jia, J., Amanai, K., Wang, G., Tang, J., Wang, B., and Jiang, J. (2002) *Nature* **416,** 548–552
37. Price, M. A., and Kalderon, D. (2002) *Cell* **108,** 823–835
38. Price, M. A., and Kalderon, D. (1999) *Development* **126,** 4331–4339
39. Zhang, W., Zhao, Y., Tong, C., Wang, G., Wang, B., Jia, J., and Jiang, J. (2005) *Dev. Cell* **8,** 267–278
40. Siegfried, E., Chou, T. B., and Perrimon, N. (1992) *Cell* **71,** 1167–1179
41. Yao, W. D., and Wu, C. F. (2001) *J. Neurophysiol.* **85,** 1384–1394
42. Ogden, S. K., Casso, D. J., Ascano, M., Jr., Yore, M. M., Kornberg, T. B., and Robbins, D. J. (2006) *J. Biol. Chem.* **281,** 7237–7243
43. Ogden, S. K., Ascano, M., Jr., Stegman, M. A., and Robbins, D. J. (2004) *Biochem. Pharmacol.* **67,** 805–814
44. Hooper, J. E., and Scott, M. P. (2005) *Nat. Rev. Mol. Cell Biol.* **6,** 306–317
45. Kalderon, D. (2004) *Curr. Biol.* **14,** R67–R69
46. Stegman, M. A., Goetz, J. A., Ascano, M., Jr., Ogden, S. K., Nybakken, K. E., and Robbins, D. J. (2004) *J. Biol. Chem.* **279,** 7064–7071
47. Aikin, R. A., Ayers, K. L., and Thérond, P. P. (2008) *EMBO Rep.* **9,** 330–336
48. Robbins, D. J., Nybakken, K. E., Kobayashi, R., Sisson, J. C., Bishop, J. M., and Thérond, P. P. (1997) *Cell* **90,** 225–234
49. Stegman, M. A., Vallance, J. E., Elangovan, G., Sosinski, J., Cheng, Y., and Robbins, D. J. (2000) *J. Biol. Chem.* **275,** 21809–21812
50. Ruel, L., Rodriguez, R., Gallet, A., Lavenant-Staccini, L., and Thérond, P. P. (2003) *Nat. Cell Biol.* **5,** 907–913
51. Ogden, S. K., Ascano, M., Jr., Stegman, M. A., Suber, L. M., Hooper, J. E., and Robbins, D. J. (2003) *Curr. Biol.* **13,** 1998–2003
52. Lum, L., Zhang, C., Oh, S., Mann, R. K., von Kessler, D. P., Taipale, J., Weis-Garcia, F., Gong, R., Wang, B., and Beachy, P. A. (2003) *Mol. Cell* **12,** 1261–1274
53. Jia, J., Tong, C., and Jiang, J. (2003) *Genes Dev.* **17,** 2709–2720
54. van Leeuwen, F., Samos, C. H., and Nusse, R. (1994) *Nature* **368,** 342–344
55. Alcedo, J., Zou, Y., and Noll, M. (2000) *Mol. Cell* **6,** 457–465
56. Motzny, C. K., and Holmgren, R. (1995) *Mech. Dev.* **52,** 137–150
57. Ascano, M., Jr., Nybakken, K. E., Sosinski, J., Stegman, M. A., and Robbins, D. J. (2002) *Mol. Cell Biol.* **22,** 1555–1566
58. Thérond, P. P., Knight, J. D., Kornberg, T. B., and Bishop, J. M. (1996) *Proc. Natl. Acad. Sci. U.S.A.* **93,** 4224–4228
59. Hortsch, M., and Goodman, C. S. (1990) *J. Biol. Chem.* **265,** 15104–15109
60. Goetz, J. A., Singh, S., Suber, L. M., Kull, F. J., and Robbins, D. J. (2006) *J. Biol. Chem.* **281,** 4087–4093
61. Shaffer, C. D., Wuller, J. M., and Elgin, S. C. (1994) *Methods Cell Biol.* **44,** 99–108

62. Ingham, P. W. (1993) *Nature* **366,** 560–562
63. Heemskerk, J., and DiNardo, S. (1994) *Cell* **76,** 449–460
64. Ascano, M., Jr., and Robbins, D. J. (2004) *Mol. Cell Biol.* **24,** 10397–10405
65. Blum, H., Beier, H., and Gross, H. J. (1987) *Electrophoresis* **8,** 93–99
66. Sambrook, J., Fritsch, E. F., and Maniatis, T. (1989) *Molecular Cloning: A Laboratory Manual.*, 2nd Ed., Cold Spring Harbor Laboratory Press, Cold Spring Harbor, NY
67. Currie, D. A., Milner, M. J., and Evans, C. W. (1988) *Development* **102,** 805–814
68. Schneider, I. (1972) *J. Embryol. Exp. Morphol.* **27,** 353–365
69. Monnier, V., Dussillol, F., Alves, G., Lamour-Isnard, C., and Plessis, A. (1998) *Curr. Biol.* **8,** 583–586
70. Norton, A. W., Hosier, S., Terew, J. M., Li, N., Dhingra, A., Vardi, N., Baehr, W., and Cote, R. H. (2005) *J. Biol. Chem.* **280,** 1248–1256
71. Riches, Z., Stanley, E. L., Bloomer, J. C., and Coughtrie, M. W. (2009) *Drug Metab. Dispos.* 10.1124/dmd.109.028399
72. Umenishi, F., Summer, S. N., Cadnapaphornchai, M., and Schrier, R. W. (2002) **62,** 2288–2293
73. Sasse, J., and Gallagher, S. R. (2009) *Curr. Prot. Mol. Biol.* **85,** 1–27
74. Ross, E. M. (1989) *Neuron* **3,** 141–152
75. Alberts, B., Johnson, A., Lewis, J., Raff, M., Roberts, K., and Walter, P. (2007) *Mol. Biol. Cell.* 5th Ed., Garland Science, New York, NY
76. Meng, X., Poon, R., Zhang, X., Cheah, A., Ding, Q., Hui, C. C., and Alman, B. (2001) *J. Biol. Chem.* **276,** 40113–40119
77. Fouix, S., Martin-Lannerée, S., Sanial, M., Morla, L., Lamour-Isnard, C., and Plessis, A. (2003) *Genes Cells* **8,** 897–911
78. Préat, T., Thérond, P., Limbourg-Bouchon, B., Pham, A., Tricoire, H., Busson, D., and Lamour-Isnard, C. (1993) *Genetics* **135,** 1047–1062
79. Dussillol-Godar, F., Brissard-Zahraoui, J., Limbourg-Bouchon, B., Boucher, D., Fouix, S., Lamour-Isnard, C., Plessis, A., and Busson, D. (2006) *Dev. Biol.* **291,** 53–66
80. Pham, A., Therond, P., Alves, G., Tournier, F. B., Busson, D., Lamour-Isnard, C., Bouchon, B. L., Préat, T., and Tricoire, H. (1995) *Genetics* **140,** 587–598
81. Lee, E., Salic, A., Krüger, R., Heinrich, R., and Kirschner, M. W. (2003) *PLoS Biol.* **1,** E10